Diagnosing and Removing CD-SEM Metrology Artifacts

Chris A. Mack[a], Gian F. Lorusso[b], and Christie Delvaux[b]

[a]*Fractilia, LLC, 1605 Watchhill Rd, Austin, TX 78703, USA*
[b]*imec, Kapeldreef, Leuven, Belgium*

Abstract

Background: Random and systematic errors found in CD-SEM tools affect the measurement of roughness in dramatically different ways than the measurement of the average critical dimension.
Aim: In order to increase the accuracy of roughness measurements, monitor the health of CD-SEM tools, and improve CD-SEM tool matching, it is important to measure and remove the impact of random and systematic errors from the measurements.
Approach: Several different CD-SEM tool systematic errors have been identified, but the scan error signature in particular was found to be very relevant. This signature is measured using the mean contour of many properly sampled features and can be used as the target edge for roughness calculations in order to remove this error.
Results: Using six different CD-SEM tools and a large data set of across-wafer, across-scanner-field measurements of the same wafer, each CD-SEM tool was found to have a unique CD-SEM signature. Subtracting off this error signature significantly improved the accuracy of the roughness measurements and the CD-SEM tool-to-tool matching. It also identified one tool as being problematic, requiring further attention.
Conclusions: Measurement and characterization of the CD-SEM scan error is a powerful tool, along with measurement and removal of random edge detection noise, for monitoring CD-SEM tool health, matching different CD-SEM tools, and improving the accuracy of line-edge and linewidth roughness measurements.

Keywords: linewidth roughness, LWR, line-edge roughness, LER, stochastics, unbiased roughness, CD-SEM, fleet matching, scan error signature

I. INTRODUCTION

The control and improvement of patterning processes in semiconductor manufacturing requires the use of many different metrology steps. For example, a critical dimension scanning electron microscope (CD-SEM) is used to measure CD and those measurements are used during process development for making process choices and for optimization, and during manufacturing for process monitoring and control. As with any measurement, errors related to CD-SEM measurements involve both random and systematic components. Random errors and variations in systematic errors result in lack of precision, and systematic errors result in lack of accuracy.

Another use of the CD-SEM besides the measurement of critical dimension is the measurement of roughness. For line/space patterns, this is the measurement of linewidth roughness (LWR) and space width roughness (SWR), line-edge roughness (LER) for both left and right edges, as well as the average of the two, and pattern placement roughness (PPR), the centerline between the left and right edges of a line. And like the measurement of CD, roughness measurements always include the impact of random and systematic errors coming from the CD-SEM. There are important differences, however, in the impact of CD-SEM errors on CD versus LWR, for example. CD is the average linewidth of a long line, whereas LWR is the standard deviation of the line's width. Random edge detection errors (with zero mean) tend to average to zero when measuring the average CD, but always bias the LWR higher.[1]

Likewise, systematic errors from the CD-SEM manifest differently for CD versus roughness. For example, distortions in the SEM field can have a large impact on the low-frequency portion of the LER power spectral density (PSD) while having no noticeable impact on mean CD.[2] Other sources of error and uncertainty coming from the CD-SEM tend almost always to have a greater impact on roughness measurement precision and accuracy than on CD measurement due to the inherent averaging that accompanies the measurement of CD.

In this study a series of very large data sets were used to carefully analyze the systematic and random contributors to errors in roughness measurements. In almost all cases, the measurement of an error enabled the removal of that error in order to improve both roughness measurement precision and accuracy. In two cases, unexpected problems were identified with different CD-SEM tools that went undetected until this roughness data was examined. In the end, significant improvement was made in the matching of multiple CD-SEM tools across multiple generations for the measurement of LER and LWR.

II. EXPERIMENTAL CONDITIONS

Much of the data used in this study came from a single wafer. This wafer, processed at imec, was exposed with a large array of 32 nm pitch lines and spaces using an NA = 0.33 EUV lithography tool and nominally uniform conditions. The resist was positive tone chemically amplified, 30nm thick with an organic underlayer. The reticle covered half of the scanner field with these line-space patterns and all measurements were made ADI (after develop inspect).

Six different CD-SEM tools were used, two each from a recent generation of tools (Gen3), the previous generation (Gen2), and an older generation (Gen1). Additionally, one of the Gen3 tools was also run in bidirectional scanning mode, where alternate imaging frames had left to right then right to left scanning directions. For each wafer, 33 fields were measured across the wafer and within each field a 7x7 array of measurements covered a large portion of the scanner half-field, for a total of 1617 images. This one wafer was measured seven times (using six different CD-SEM tools plus the bidirectional scan run). Each measurement run shifted the measurement position sufficiently so that no spot on the wafer was measured twice (or exposed to electrons from the CD-SEM expect during measurement).

Images were 2048X2048 pixels with a pixel size of 0.8 nm X 0.8 nm. For the Gen1 tools, the pixel size was slightly different, at 0.824 nm X 0.824 nm. This resulted in about 50 lines and spaces within the field of view of each SEM image, for a total of about 77,000 lines measured per metrology pass. All images were taken at 500V and 16 frames of averaging. Images were measured offline using MetroLER v2.2.7 from Fractilia with default parameters unless otherwise noted (FILM edge detection with no image filtering was used throughout). An example showing the across-wafer layout of the measurements is shown in Figure 1.

Additional images made using other wafers and one of the same metrology tools will be described as they are introduced in following sections.

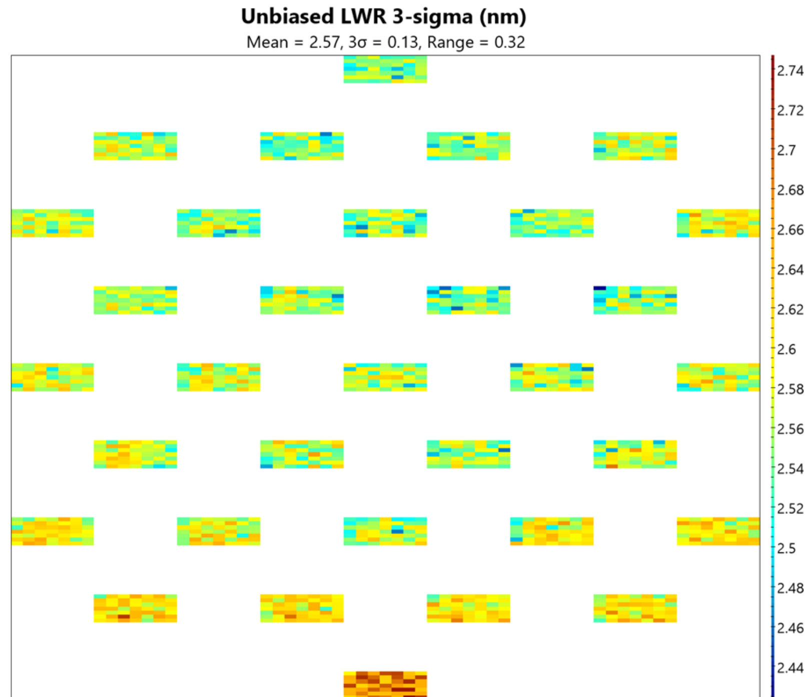

Figure 1. Example result of the 1617 images measured for one metrology pass from one CD-SEM tool.

III. ANAMOLOUS LEFT-RIGHT EDGE CORRELATIONS AND THE MEAN CONTOUR

The initial purpose of the very large data sets being collected in this study was to carefully characterize the across-field and across-wafer variations in feature roughness and to assess tool-to-tool matching between metrology tools. It was in this latter context that the first CD-SEM metrology artifact was observed. Each batch of 1617 images were analyzed in MetroLER, and in addition to batch-average metrology results and spatial variations (such as in Figure 1), image -to-image repeatability can also be assessed. As one of many metrics per image, the correlation between the left-edge and right-edge of each feature is calculated and averaged per image. The image-to-image variations can then be plotted, as in Figure 2. Shown are the results for two CD-SEM tools, a) Gen2-2 and b) Gen2-1. The Gen2-2 tool in a) shows the expected behavior of about zero correlation for every image, whereas the Gen2-1 tool in b) shows a higher baseline correlation of about 0.06 and occasional images with much higher correlations. Since the features were printed with single exposure EUV, the wafer patterns are not expected to have any correlation from left edge to right edge of the lines.

Recall that both sets of measurements are from the same wafer, so that the higher correlations from the Gen2-1 tool would seem to be a measurement anomaly, prompting further investigation. A wafer map of the line edge-edge correlation did not show any spatial signature. A portion of the image having the worst-case correlations is shown in Figure 3, along with a plot of the LER power spectral density (PSD) averaged for the 50 features of that image. Artificial zig-zags at a period of about 8 nm (10 pixels) are slightly visible in the image, corresponding to the largest spike seen in the biased LER PSDs. Interestingly, the LWR PSD for this image shows completely expected behavior with no spikes. Additionally, the images with the highest edge-edge correlations also showed higher biased LER, up to 16% higher than the average. While the worst-case image is shown in Figure 3, every image coming from the Gen2-1 tool produced LER PSDs with very noticeable spikes.

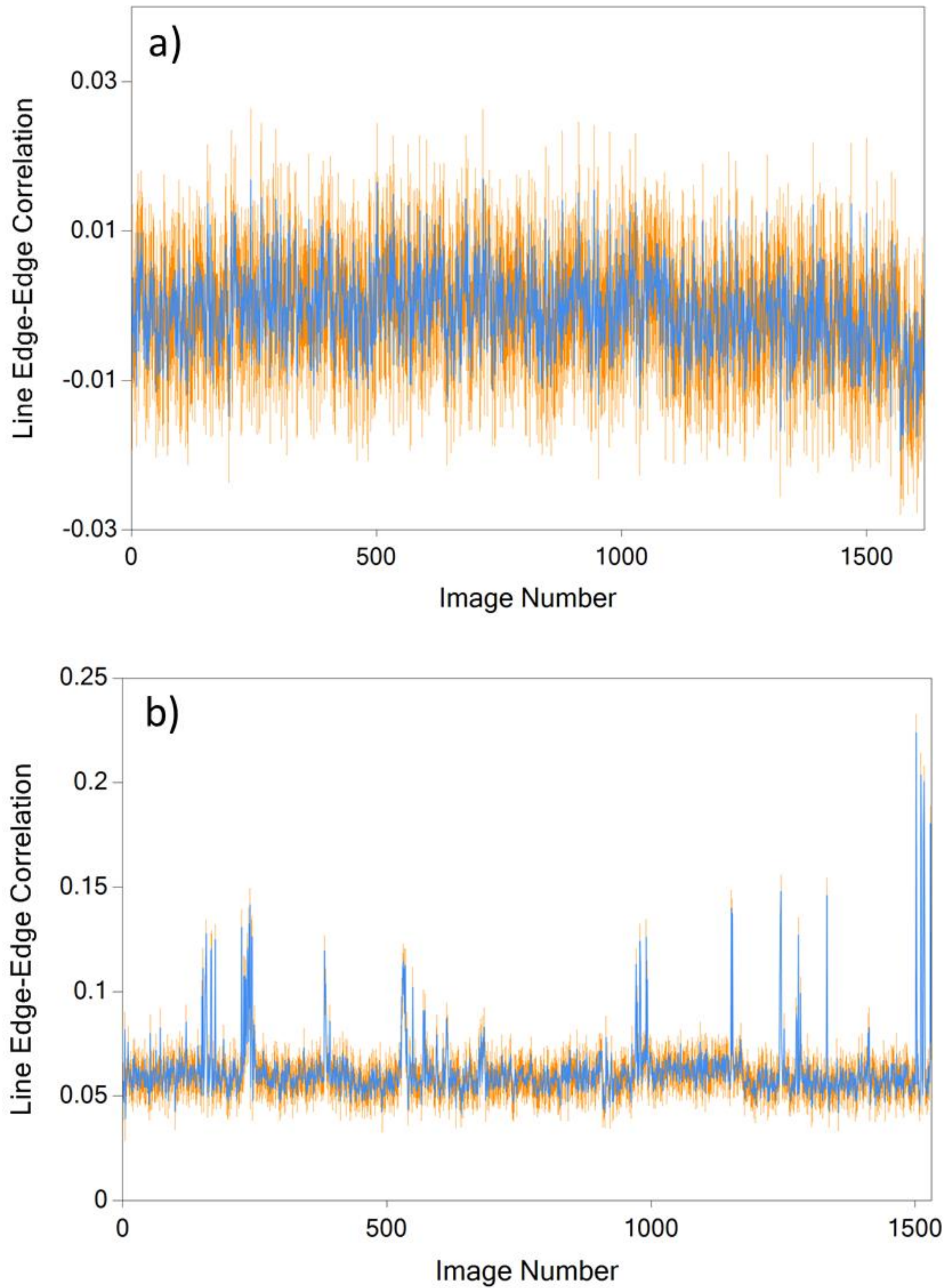

Figure 2. The image-to-image variations in left-to-right edge correlations (value in blue with error bars in orange) of the line features for two CD-SEM tools, a) Gen2-2 and b) Gen2-1, measured for the same wafer. The Gen2-2 tool in a) shows the expected behavior of about zero correlation, whereas the Gen2-1 tool in b) shows a higher baseline correlation of about 0.06 and occasional images with much higher correlations.

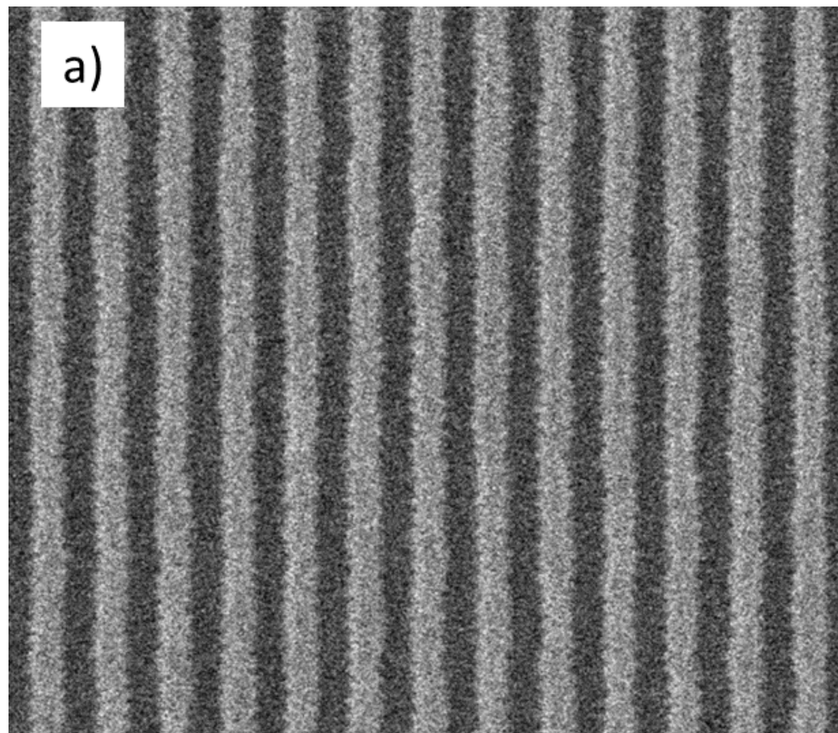

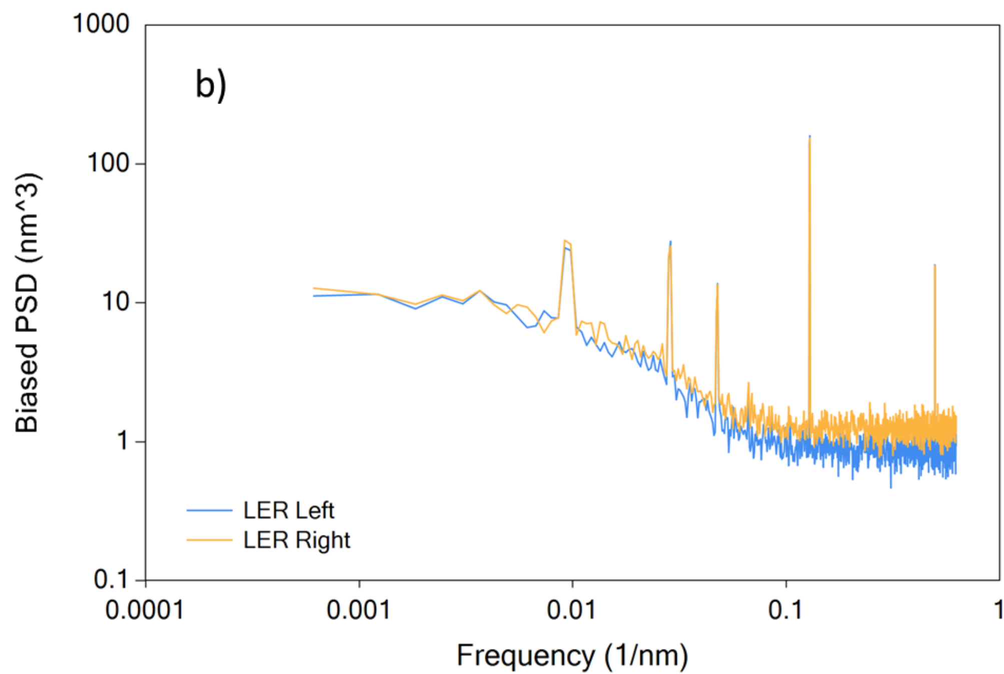

Figure 3. a) A portion of the image exhibiting the highest edge-edge correlations showing an artificial zig-zag appearance of some line edges, and b) the left and right biased LER PSDs averaged for the 50 features of this image showing large spikes at specific frequencies.

The root cause of the anomalous PSD spikes and edge-edge correlations became apparent by examining the mean contours of every feature from every image per metrology tool. The mean contours are calculated by aligning then averaging the detected edges of each feature. Because these images come from all over the wafer and at many different positions in the scanner field, things like normal lithography variations, mask variations, stochastic variations (such as LER), and edge detection noise will average away to approximately zero. What is left is the systematic scan errors of the metrology tool. Thus, the mean contours of a large number of features when sampled in such a way that only the CD-SEM behavior is constant provides a measurement of the systematic scan errors of the CD-SEM whenever those scan errors exhibit a constant phase from top to bottom of the image. The mean contours for the Gen2-1 tool are shown in Figure 4. The scan error signature of this CD-SEM is striking.

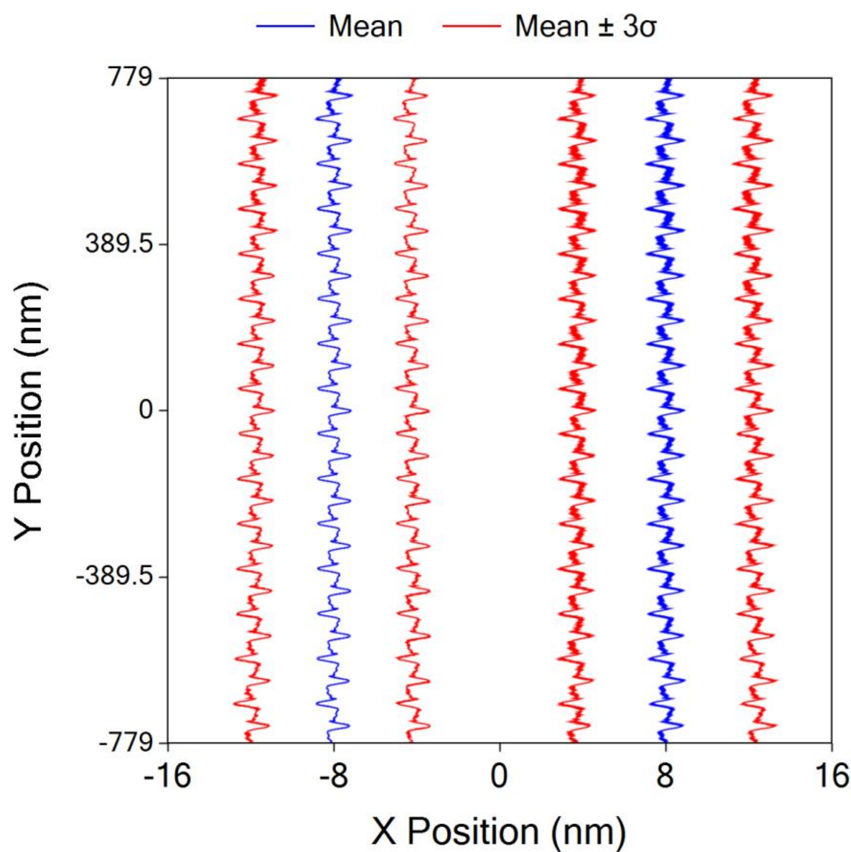

Figure 4. The mean contours (in blue) as well as mean ± 3σ contours (in red) after averaging every edge from every image from the Gen2-1 tool. A clear pattern emerges that could not be present on the wafer. Note that the x-axis and y-axis are plotted on very different scales.

The CD-SEM works by electronically scanning a beam of electrons across a stationary sample using deflectors that scan first an entire row of pixels, then shift down one pixel in y and repeat for the next row of pixels. An important component of the accuracy of the position of a detected feature edge is the accuracy with which the beam is placed at the center of every given pixel position. Errors in beam placement will result directly in errors in the detected edge position. For vertical lines and spaces, it is the x-position accuracy of the beam that has the major impact on edge detection accuracy. Deviations of the mean edge

contours as shown in Figure 4 can be interpreted as a measurement of scan errors, systematic errors in the x-placement of the beam position.

Figure 5 shows the mean left edge contours from several different CD-SEM tools (the tools not shown exhibited similar behavior). Again, for the sampling plan used here an ideal SEM tool would show a perfectly flat mean edge contour. Instead, the Gen3-2 tool showed about a 0.6 nm range of edge variation, the Gen2-2 tool showed a 0.4 nm edge variation, and the Gen1-1 tool showed about a 0.5 nm edge variation. The specific variation (signature) was unique to each tool. Note that this level of systematic scan error would be well hidden by normal line-edge roughness when looking at any single edge. For the Gen3-2 tool run in bidirectional scan mode (Figure 5b) the systematic scan error was much smaller, with a range of only about 0.1 nm. For the problematic Gen2-1 tool, as shown in Figure 4 and Figure 5d, the variation along the edge was about 1.7 nm.

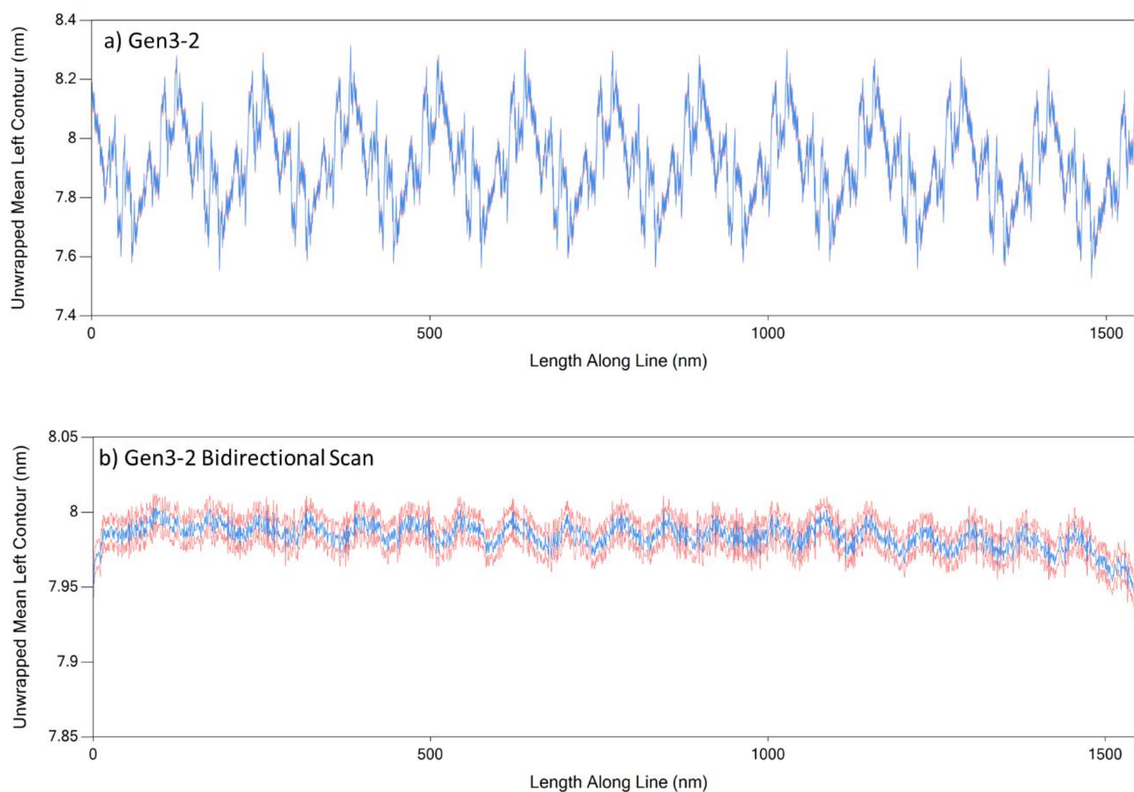

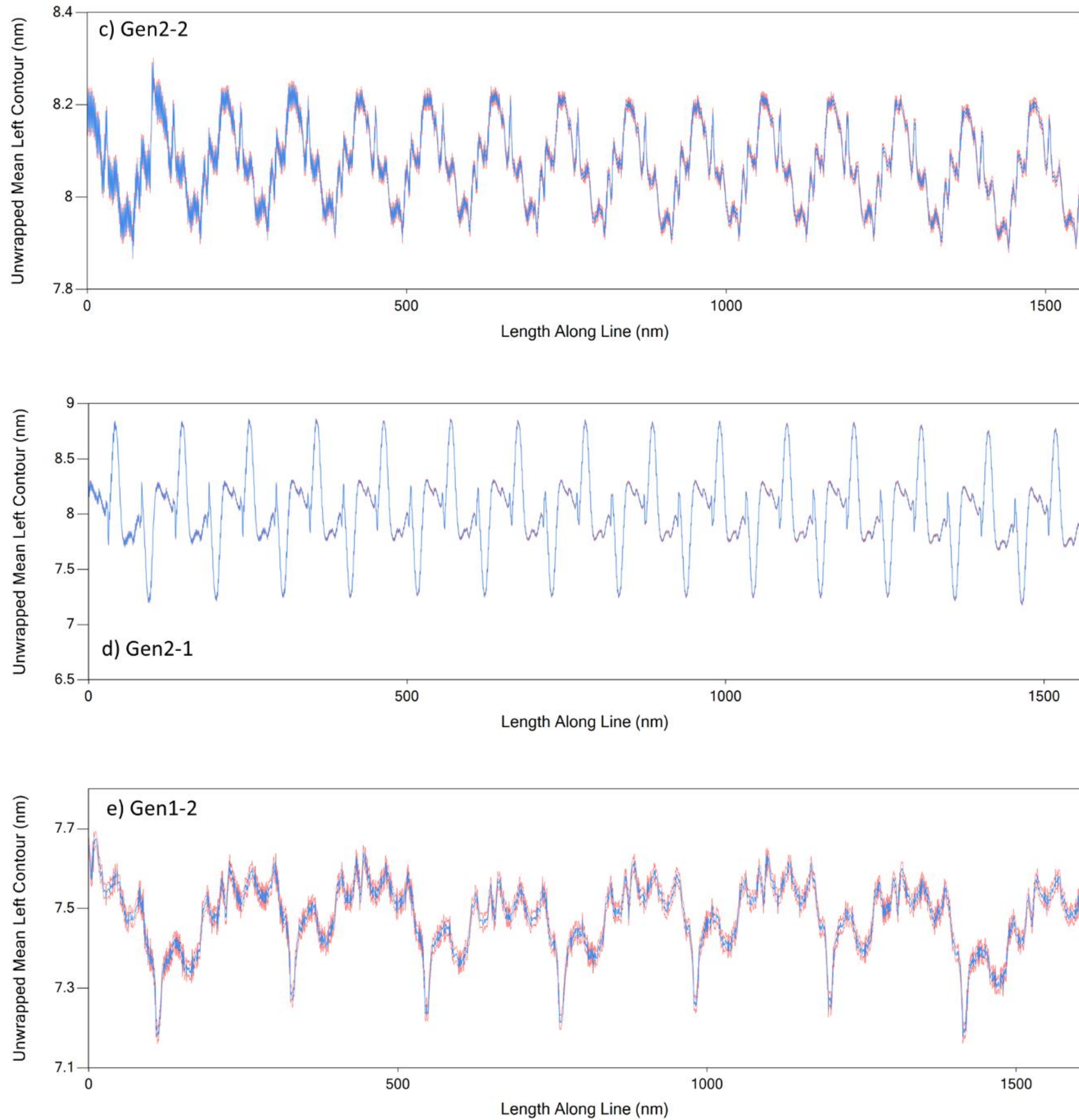

Figure 5. Examples of the mean left contours showing the unique scan error signatures of several different metrology tools. Solid blue lines show the mean contour and dashed red lines show the 95% confidence interval about that mean.

While Figure 5 shows the left edge mean contours, the right edge mean contours were similar, though not exactly the same. The mean linewidth variation from top to bottom of the lines can also be calculated and plotted in the same way and was much smaller for every CD-SEM tool, typically only 0.1 – 0.2 nm. As a result, the LER PSDs exhibited spikes in every case resulting from the systematic scan errors, but usually the LWR did not. A closer look, however, revealed another interesting phenomenon seen on some but not all tools. Figure 6 shows a portion of the mean linewidth behavior of the Gen3-2 tool with a systematic oscillation of linewidth from pixel row to pixel row. While less than 0.1 nm in magnitude, this oscillation produces a pronounced spike in the LWR PSD at the Nyquist frequency.

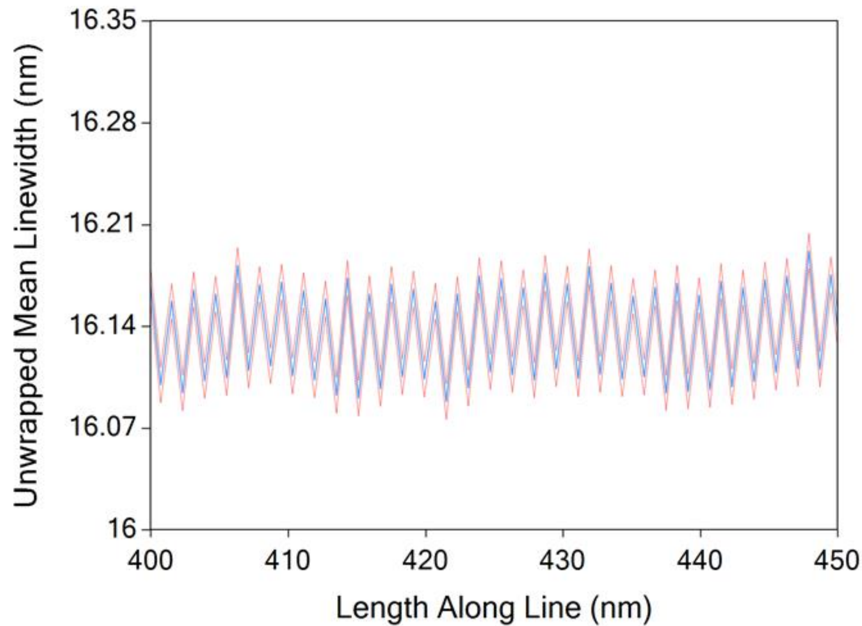

Figure 6. A close-up look at the mean linewidth behavior of the Gen3-2 tool shows a systematic oscillation of linewidth from pixel row to pixel row, producing a spike in the LWR PSD at the Nyquist frequency. Solid blue line shows the mean contour and dashed red lines show the 95% confidence interval about that mean.

The mean contours, when found by averaging a sufficient number of features and sampling in such a way as to average away all other possible systematic errors, provides a valuable measure of the scan errors of the CD-SEM tool. As the results above show, each CD-SEM tool has a unique scan error signature. Additionally, the scan error signature can vary depending on the settings of the CD-SEM, but is consistent at least when measuring multiple wafers from the same lot. Figure 7 shows three wafers from one lot measured on the Gen2-2 tool, showing a consistent scan-error signature. Figure 8 shows that changing the pixel size and shape from square to rectangular produces a different scan error signature. By plotting the 95% confidence intervals around each mean contour it is clear when the observed scan error signatures are statistically significant.

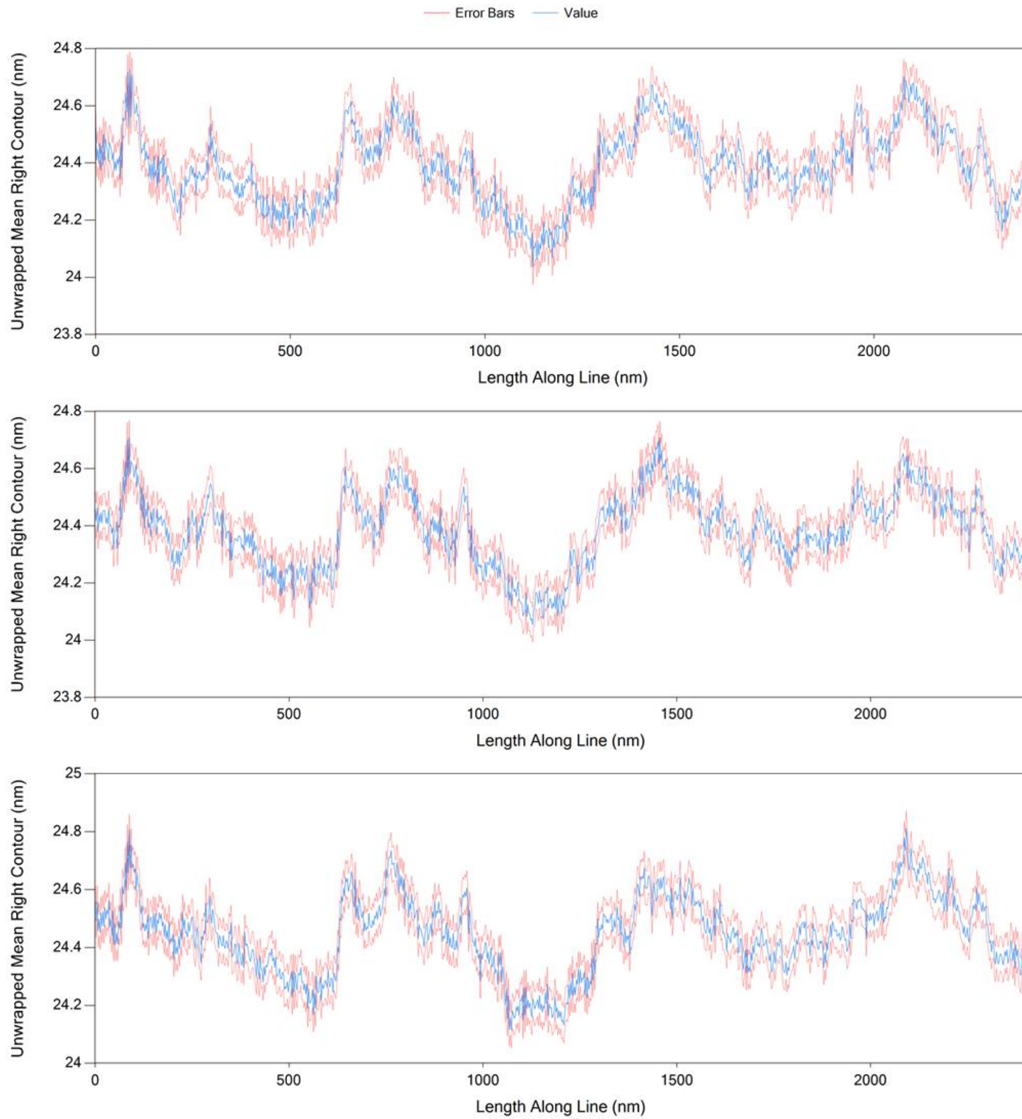

Figure 7. Mean right contours measured from three wafers from the same lot. About 90 images per wafer were measured, averaging about 2200 features per mean contour. In this case, rectangular pixels were used (0.88 nm X 2.5 nm) on 1024 X 1024 images. The mean contour is in solid blue and the 95% confidence interval about the mean is in dashed red.

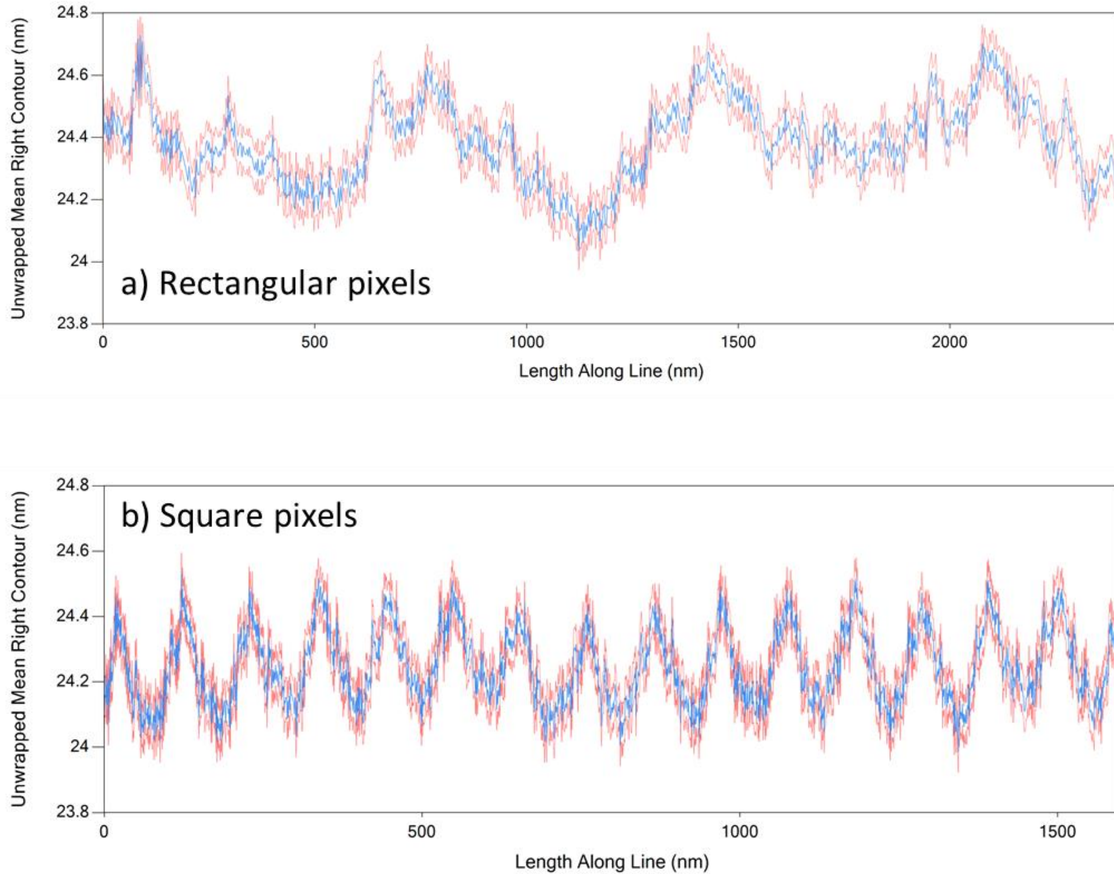

Figure 8. Mean right contours measured using the same CD-SEM tool from different wafers and different lots on different days: a) rectangular pixels (0.88 nm X 2.5 nm) on 1024 X 1024 images, and b) square pixels (0.8 nm X 0.8 nm) on 2048 X 2048 images. The mean contour is in solid blue and the 95% confidence interval about the mean is in dashed red.

IV. MITIGATING THE EFFECT OF THE SCAN ERROR SIGNATURE

The scan error signature is a valuable tool for characterizing a specific CD-SEM tool and assessing its health. For example, the problematic Gen2-1 CD-SEM tool was in use at imec and this problem was not caught until the mean contour analysis shown above was performed. Further, the impact of these CD-SEM systematic scan errors can be mitigated by using mean contour detrending. The LER and LWR of a feature (and their PSDs) are calculated by first subtracting the measured edge from a target edge to get an edge error (a process called detrending). Typically, the target edge used is an ideal edge, such as a best-fit straight line for LER or the mean linewidth for LWR. But more generally any target edge can be chosen. If the mean contour is used as the target edge then the impact of CD-SEM scan errors can be mitigated. Figure 9 shows PSDs calculated for the Gen2-1 tool using both ideal edge detrending and mean contour detrending. Almost all of the anomalous spikes in the PSDs are removed when mean contour detrending is used. Note that some residual spikes remain, probably because of the somewhat inconsistent nature of the scan errors for this problematic tool (see Figure 2b).

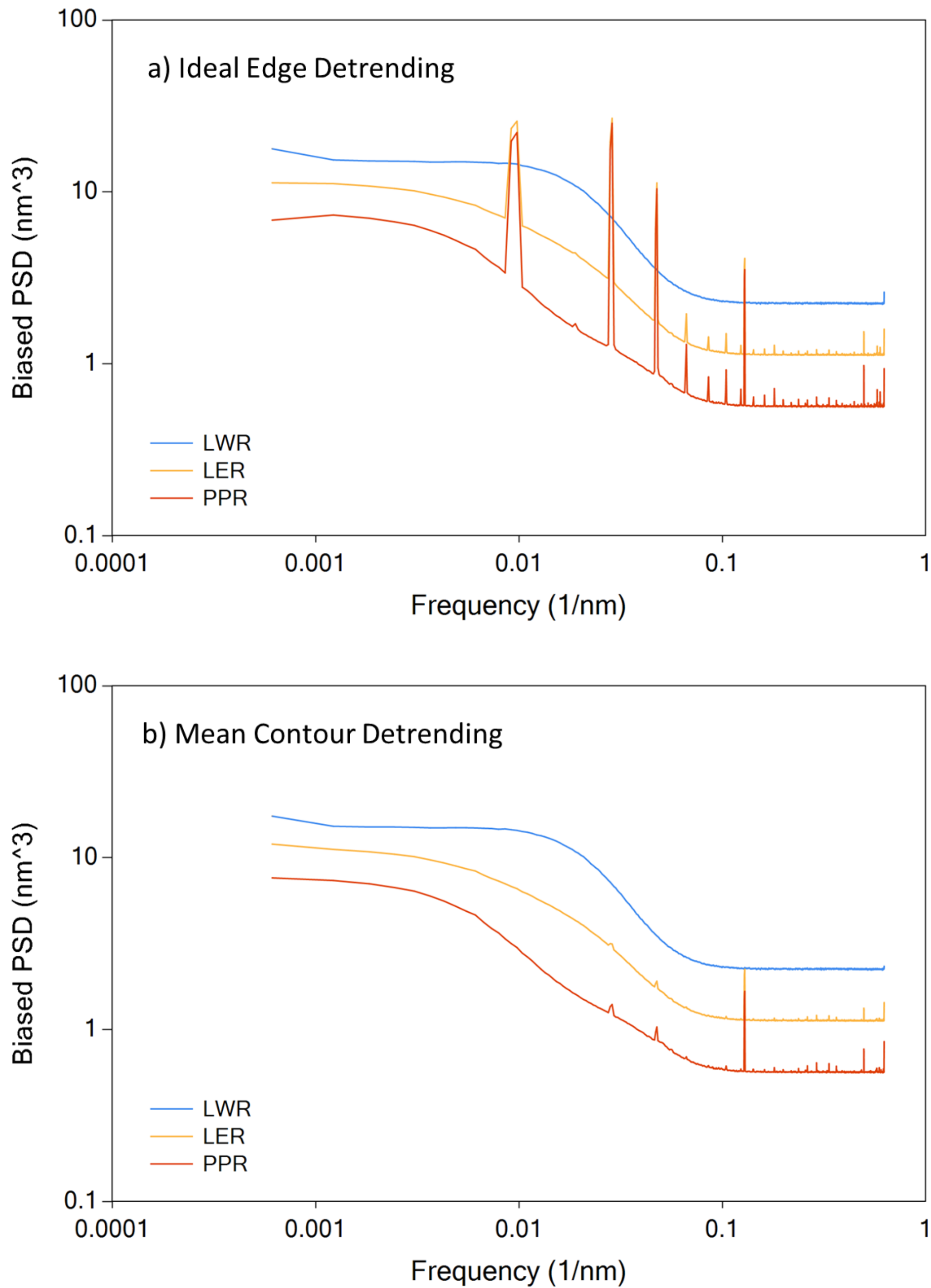

Figure 9. Impact of detrending choice on the PSDs for the Gen2-1 tool: a) typical ideal edge detrending showing large spikes in the LER and PPR PSDs caused the systematic scan errors, and b) mean contour detrending that eliminates most of the PSD spikes.

While less dramatic, similar effects are seen when using mean contour detrending for the other CD-SEM tools. Each systematic scan error signature includes various periodic behaviors (see Figure 5), resulting in spikes in the LER PSD and higher 3σ LER. Using mean contour detrending removes these spikes and produces a more accurate LER measurement. Note that the mean contour only captures systematic scan errors that exhibit a constant phase from top to bottom of the image for every image. If, for example, a scan error source produced a sinusoidal variation in detected edge position for each image, but the phase of that error varied randomly image to image, the error would average away when calculating the mean contour. The result would be a spike in the PSD (set by the period of the scan error) that would not be removed by mean contour detrending.

Finally, mean contour detrending can be used for improved matching of CD-SEM tools. Since each scan error signature is unique to each CD-SEM tool, mean contour detrending will help to make each tool more consistent with each other. The results of CD-SEM tool matching will be shown in a subsequent section.

V. ANAMOLOUS AUTOFOCUS BEHAVIOR FOR THE OLDER GENERATION CD-SEM TOOLS

Another interesting metrology artifact was observed for the oldest generation CD-SEM tools used in this study. Again, the anomalies were discovered by looking at the image-to-image behavior for the large across-wafer study (roughly equivalent to trend-charting various metrology outputs). The biased LWR for the Gen1 tools was consistently 2X higher (about 11 nm) than for the Gen2 and Gen3 tools (about 5.5 nm) due to the poorer image quality of the Gen1 tools and subsequent greater bias in LWR measurement. However, occasionally the biased LWR was seen to be much higher (as high as 20 nm), as shown in Figure 10. Looking at the images associated with the anomalously high biased LWR values shows a clearly degraded image. Again, since the same wafer was measured at multiple locations by multiple CD-SEM tools, it is unlikely that this behavior is actually present on the wafer. Instead, it seemed to be an imaging problem with the CD-SEM, and probably an autofocus problem.

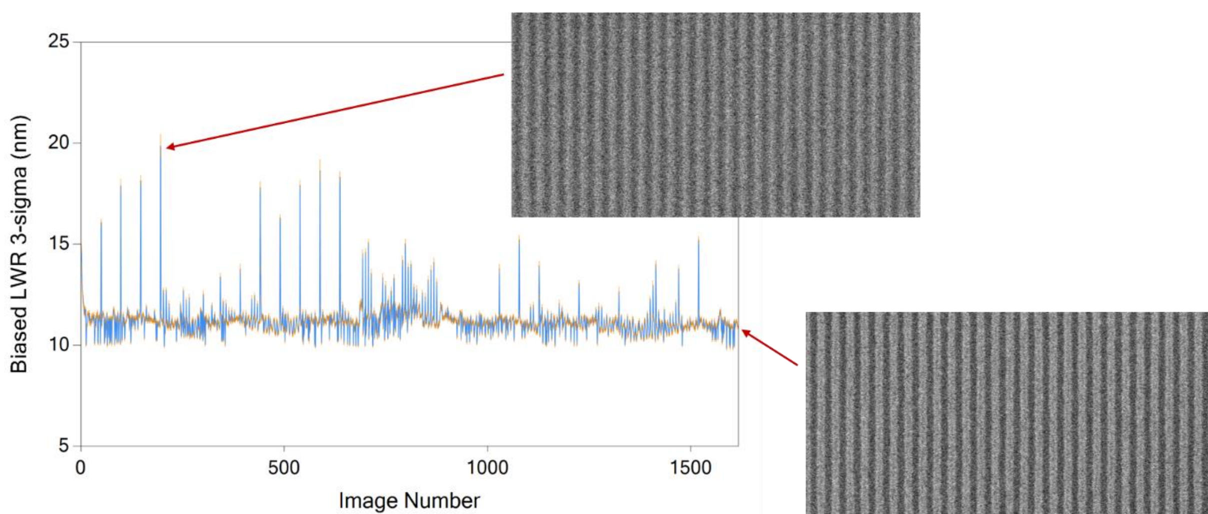

Figure 10. Some images measured on the Gen1-2 tool appear to be out of focus. Similar results were seen on the Gen1-1 tool, though with fewer out-of-focus images.

Further investigation showed a specific spatial distribution of these higher biased LWR values across the scanner field, as seen in Figure 11. By examining the CD-SEM measurement recipe, the specific order of measurements is plotted out in Figure 12, giving a clue as to what might be happening. It appears that the autofocus failure occurs after a long stage travel, with the worst behavior occurring for the longest stage travel, that between chip fields.

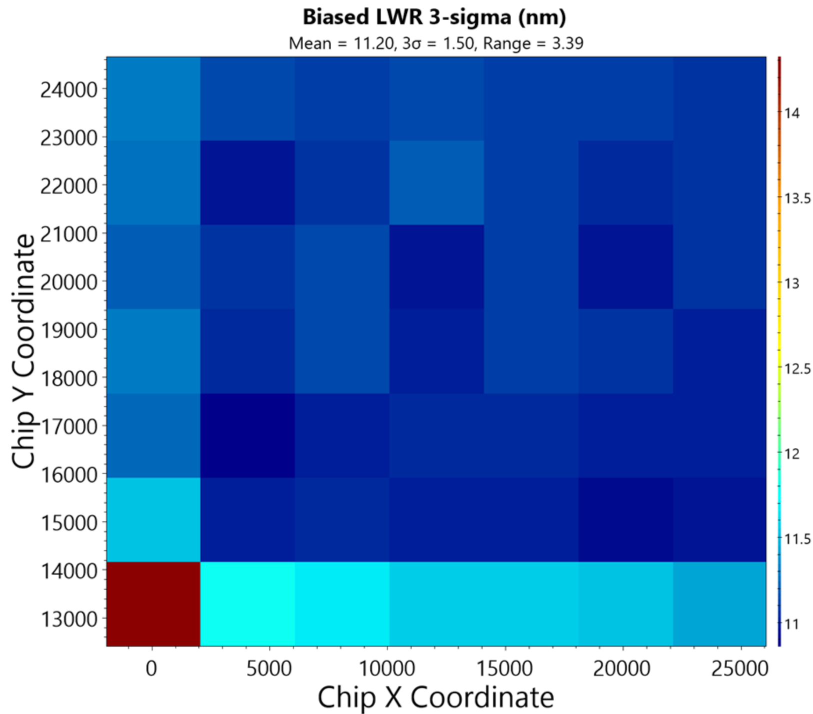

Figure 11. The average of all scanner field measurements across the wafer indicates that the LWR measurement is highest at the corner of the field.

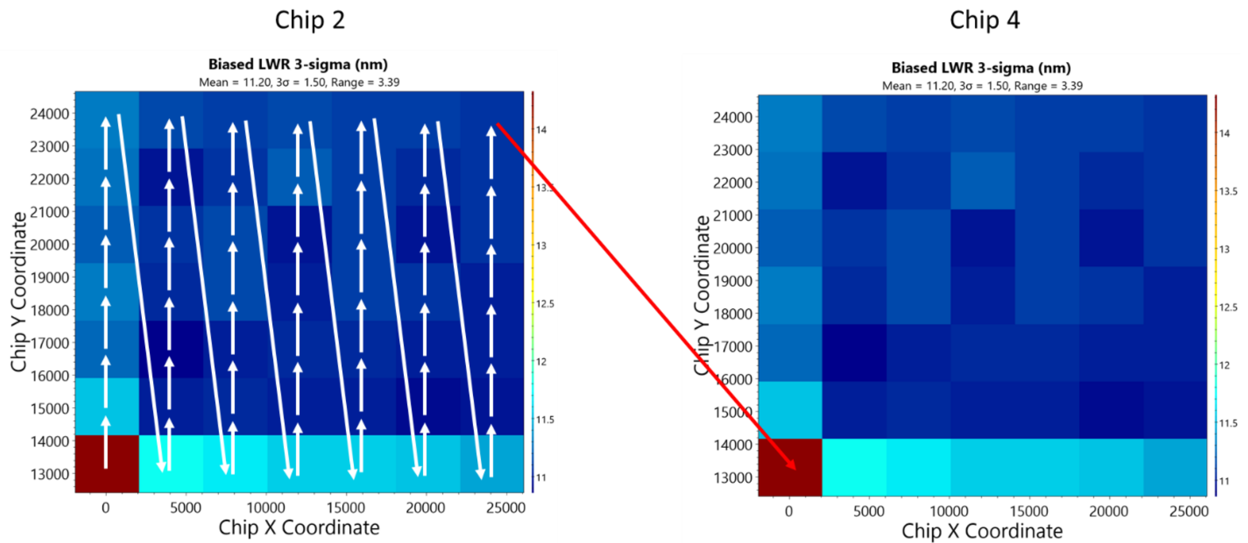

Figure 12. Plotting the motion of the CD-SEM stage as measurements are taken within one chip field and from chip field to chip field provides a clue that an autofocus failure occurs after long stage travel.

To investigate the possible mitigation of the autofocus failures, each image was analyzed separately instead of as a batch. To calculate the unbiased LWR, the metrology noise floor of the average PSD is first calculated, in this case using the average of each feature per image. Figure 13 shows two such image-average PSDs for a typical and out-of-focus image. The higher noise floor for the out-of-focus image is evident. Since the higher noise floor can be removed using the standard procedure for unbiasing the LWR,[3-6] it is possible that even the out-of-focus images could produce a reliable unbiased LWR measurement. Figure 14 shows the unbiased LWR values corresponding to the biased LWR values seen in Figure 10. For images with biased LWR values between 10 – 20 nm, all but one image produced a very consistent unbiased LWR of about 2.4 nm. Only the worst-case image, with a biased LWR value of 20 nm, failed to provide adequate unbiasing of the LWR.

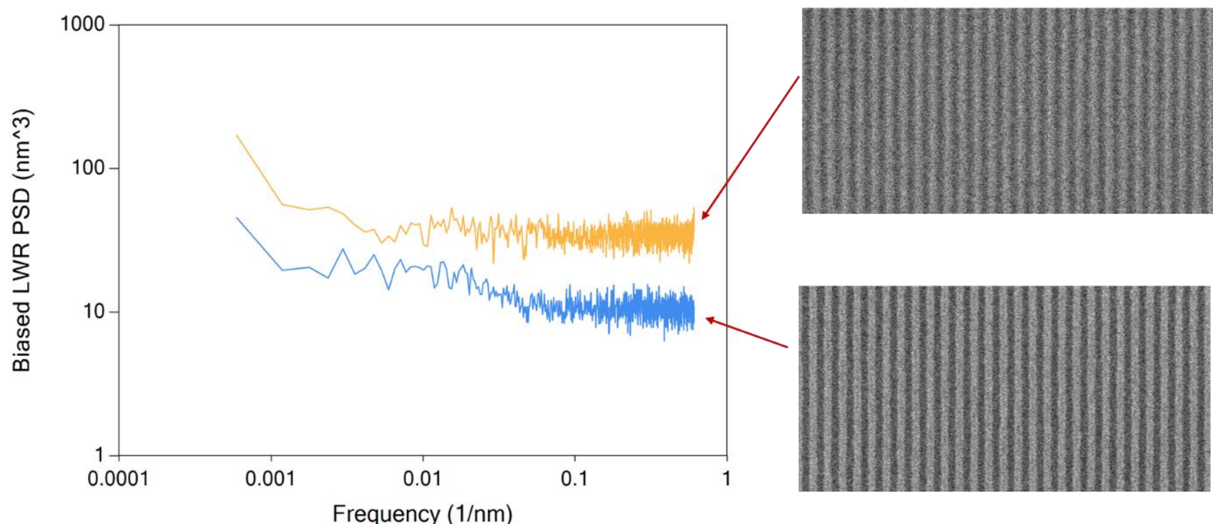

Figure 13. Biased LWR PSDs for a "good" and "bad" image from the Gen1 tool, indicating that the poorly focused image has higher metrology noise (the high-frequency plateau of the PSD).

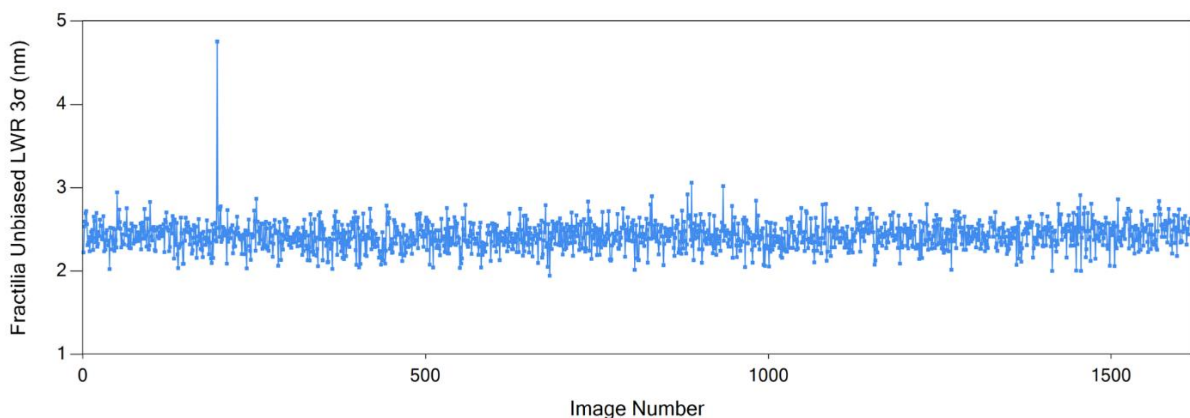

Figure 14. Unbiased LWR calculated on an image-by-image basis for the same images shown in Figure 10. For images with biased LWR values between 10 – 20 nm, all but one image produced a very consistent unbiased LWR of about 2.4 nm.

VI. CD-SEM TOOL MATCHING

While the above sections detail two very specific CD-SEM metrology artifacts, there are other sources of systematic metrology errors present in every CD-SEM image. Variation is the background grayscale intensity level, especially top to bottom, will produce a CD variation that will appear as low-frequency roughness for both LER and LWR. Standard field flattening approaches can be used on an image-by-image basis, and any SEM field non-flatness that is consistent across all images can also be removed by mean contour detrending. Distortions of the SEM image field, including things like trapezoidal and pincushion distortion, will result in increases in the low-frequency LER PSD. When averaging many SEM images together, these distortions can be measured and removed.

By using every available means to measure and remove systematic and random errors caused by the CD-SEM, the best possible unbiased LER and LWR can be obtained, with one goal being a better matching of CD-SEM tools. Figure 15 shows the biased LWR for the different metrology tools measuring the same wafer. The full range of biased LWR values in 110%, mostly due to the very high bias found in the oldest generation CD-SEMs. For the Gen2 and Gen3 tools, the range of biased LWR values is 8%. By unbiasing the LWR and removing each of the systematic CD-SEM errors discussed above, the range of unbiased LWR values is reduced to 6%. Considering only the Gen2 and Gen3 tools, the range is reduced to 1.8% (Figure 16). In absolute terms, the Gen2 and Gen3 tools produced a range of biased LWR values of 0.4 nm for the same wafer, whereas the unbiased LWR values exhibited a range ten times less, 0.04 nm. The results for LER are very similar: for the Gen2 and Gen3 tools the biased LER range of 11% was reduced to an unbiased range of 2%.

VII. CONCLUSIONS

Measurement of line-edge roughness and linewidth roughness in a top-down CD-SEM is impacted by both random and systematic errors coming from the SEM. Random errors generally take the form of edge detection noise, which is removed in the process of converting a biased LER or LWR measurement to unbiased values. Systematic errors take many forms and so should be addressed at different points in the edge detection and analysis process as appropriate. In this study, the discovery of a CD-SEM tool problem led to a general approach to measure and subtract out systematic scan errors.

These scan errors are measured as the mean contour, the average of every feature's detected edges, when the experimental conditions are such that the only systematic errors in the mean contour are the scan errors in the CD-SEM tool. This is accomplished first by having sufficient numbers of features (printed from a nominally uniform array of features) averaged together so that stochastic variations are averaged away, and also by sampling at multiple places in the field so that mask errors, proximity effects, and other systematic variations from top to bottom of the features will not be present. Calculating and displaying the confidence interval about the mean contour helps ensure that the observed scan errors are statistically significant and that a sufficient number of features have been averaged together to produce a meaningful result.

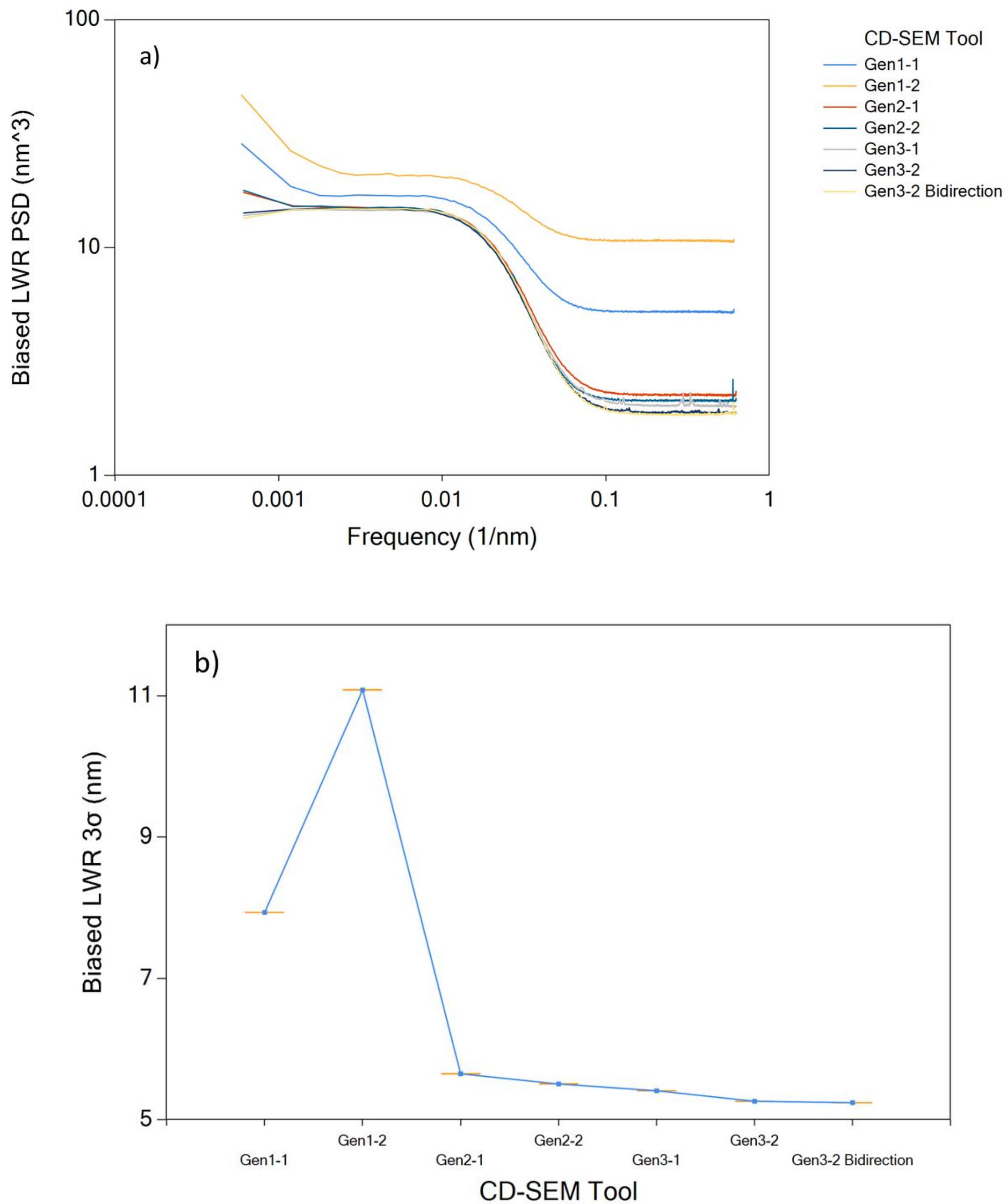

Figure 15. Biased LWR measurements of the same wafer made using six different CD-SEM tools: a) biased PSDs and b) biased LWR. For all tools, the range of biased LWR values is 110%. For the Gen2 and Gen3 tools, the range of biased values is 8% (0.4 nm).

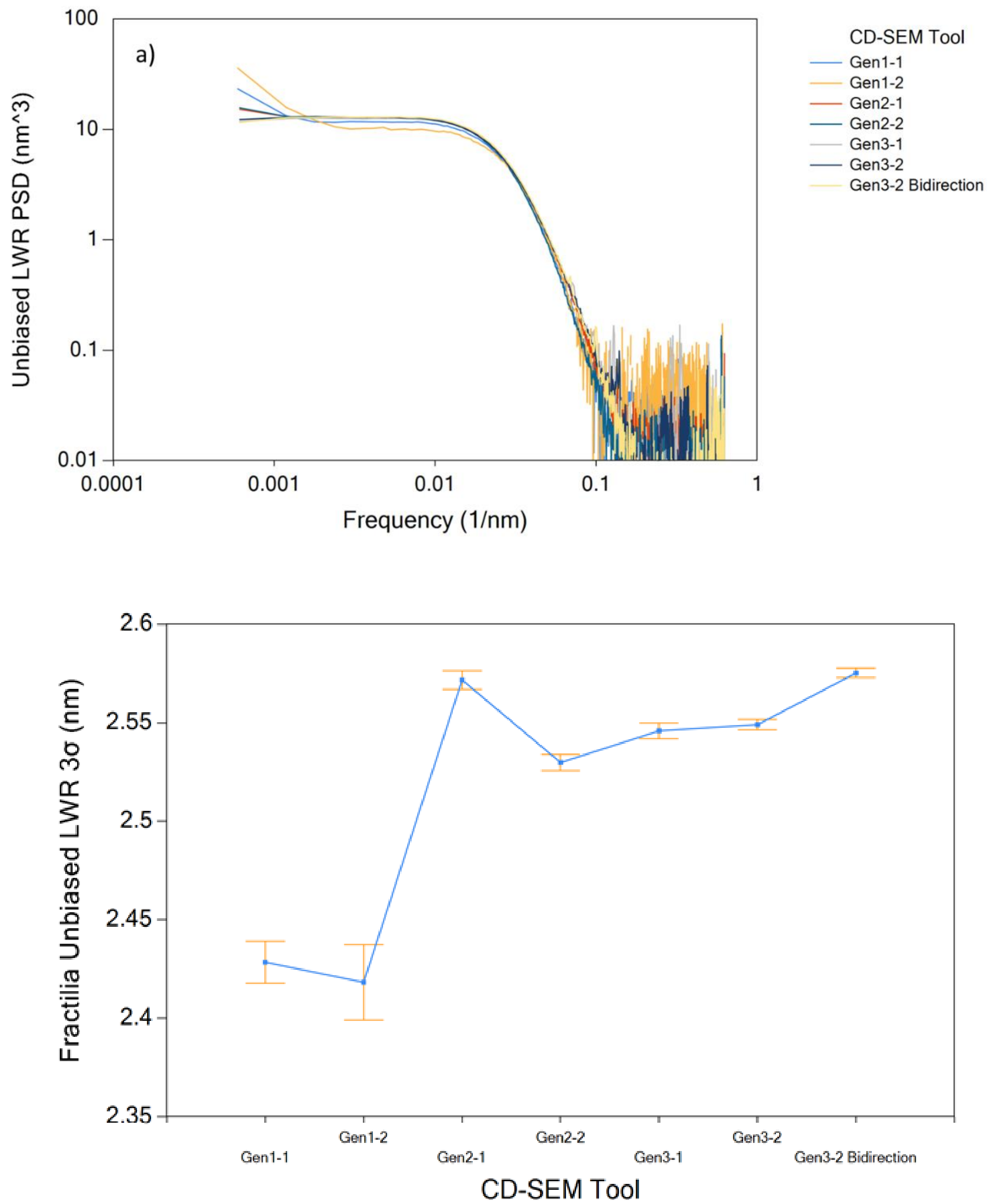

Figure 16. Unbiased LWR measurements of the same wafer made using six different CD-SEM tools: a) unbiased PSDs and b) unbiased LWR. For all tools, the range of unbiased LWR values is 6%. For the Gen2 and Gen3 tools, the range of unbiased values is 1.8% (0.04 nm).

As observed for six different CD-SEM tools, plus one tool run in a bidirectional scan mode, each tool exhibited a unique scan error signature. The bidirectional scan mode showed significantly reduced but still noticeable scan errors. The scan error signature was seen to be stable for one tool at least over a short period of time, but changed when the pixel shape was changed from square to rectangular. This preliminary look at the characteristics of the scan error signature should be expanded into a more detailed study of what CD-SEM parameters affect the signature.

Three uses of the CD-SEM scan error signature have been identified. First, the signature can be used to monitor the health of the CD-SEM tool. In this study, one CD-SEM exhibited a signature with excessively large variation, requiring maintenance. Second, subtracting the scan error signature by using the mean contour as the target edge of LER and LWR calculation leads to more accurate roughness measurement. And finally, removing the signature from different CD-SEM tools leads to better matching of roughness measurements between tools. In general, the three benefits stated here for scan error signature measurement also apply to other random and systematic errors in CD-SEM tools as well.

While the mean contour concept has been shown here for lines and spaces, it can also be applied to other feature types, though with somewhat different interpretations. For example, for contact holes, the mean shape of the holes may not be perfectly circular. Using the mean contour for detrending rather than the ideal circular shape separates the measurement of shape errors from the measurement of LER.

References

[1] J. Villarrubia and B. Bunday, "Unbiased Estimation of Linewidth Roughness", *Metrology, Inspection, and Process Control for Microlithography XIX*, Proc. SPIE Vol. 5752, 480-488 (2005).

[2] Barton Lane, Chris Mack, Nasim Eibagi, and Peter Ventzek, "Global minimization line-edge roughness analysis of top down SEM images", *Metrology, Inspection, and Process Control for Microlithography XXXI*, Proc. SPIE Vol. 10145, 101450Y (2017).

[3] Chris A. Mack, "Reducing roughness in extreme ultraviolet lithography," *J. Micro/Nanolith. MEMS MOEMS*, **17**(4), 041006 (2018).

[4] Gian F. Lorusso, Vito Rutigliani, Frieda Van Roey, and Chris A. Mack, "Unbiased Roughness Measurements: Subtracting out SEM Effects", *Microelectronic Engineering*, **190**, 33–37 (2018).

[5] Gian F. Lorusso, Vito Rutigliani, Frieda Van Roey, and Chris A. Mack, "Unbiased Roughness Measurements: Subtracting out SEM Effects, part 2", *Journal of Vacuum Science & Technology B*, **36**(6), 06J503 (2018).

[6] Chris A. Mack, Frieda Van Roey, and Gian F. Lorusso, "Unbiased Roughness Measurements: Subtracting out SEM Effects, part 3", *Metrology, Inspection, and Process Control for Microlithography XXXIII*, Proc. SPIE **10959**, 109590P (2019).